Malaysian Journal of Analytical Sciences (MJAS)



Published by Malaysian Analytical Sciences Society

PEROXYMONOSULFATE ACTIVATION USING NITROGEN-DOPED BIOCHAR FOR ACID ORANGE 7 REMOVAL IN WATER

(Pengaktifan Peroksimonosulfat dengan Bioarang Terdop Nitrogen untuk Penyingkiran Asid Oren 7 dalam Air)

Mohamed Faisal Gasim, Nivethah Sivam, and Wen-Da Oh*

School of Chemical Sciences, Universiti Sains Malaysia, 11800 Penang, Malaysia

*Corresponding author: ohwenda@usm.my

Received: 18 August 2023; Accepted: 21 December 2023; Published: 28 February 2024

Abstract

In this study, N-doped plastic-derived biochar was synthesized at different synthesis temperatures (600, 700 and 800 °C) using a facile one-pot pyrolysis technique. The as-prepared N-doped biochars were employed to investigate the effect of pyrolysis temperature on the biochar characteristics and catalytic performance as peroxymonosulfate (PMS) activator for acid orange 7 (AO7) removal. The X-ray Diffraction (XRD) analysis indicated that the N-doped biochar consists of amorphous carbon whereas the field emission scanning electron microscope (FESEM) images illustrated that the catalysts have microparticles morphology with porous features. The N-doped biochar synthesized at 800 °C (N-800) displayed the best performance with 98% AO7 removed in 30 min (pseudo first-order rate constant, $k_{app} = 0.211 \text{ min}^{-1}$). The k_{app} was positively affected by increasing the PMS dosage and N-800 loading while neutral condition (pH = 7) was optimum for AO7 removal. The scavenger study suggests that singlet oxygen ($^{1}O_{2}$) was the dominant reactive oxygen species (ROS) in this reaction system as sodium azide (NaN₃) scavenger inhibited the AO7 removal by 80%. N-800 catalytic performance in removing AO7 was reduced from 97 to 22% after four consecutive cycles due to irreversible adsorption and oxidation of active sites. Overall, the N-800 was able to activate PMS effectively with a promising potential for sustainable azo dye removal. Future-wise, the employment of co-doping other heteroatoms (such as S, B) into N-doped plastic-derived biochar for synergistic effects should be investigated.

Keywords: advanced oxidation process, peroxymonosulfate, acid orange 7, nitrogen doping, biochar

Abstrak

Dalam kajian ini, bioarang terdop N telah disintesis daripada plastik pada suhu sintesis yang berbeza (600, 700 dan 800 °C) dengan menggunakan teknik pirolisis satu periuk. Bioarang terdop N yang disediakan telah digunakan untuk menyiasat kesan suhu pirolisis ke atas ciri-ciri bioarang dan prestasi sebagai pemangkin bagi pengaktifan peroksimonosulfat (PMS) untuk penyingkiran asid oren 7 (AO7). Analisa pembelauan sinar-X menunjukkan bioarang terdop N terdiri daripada karbon amorfus manakala mikroskop elektron pengimbasan pelepasan medan (FESEM) menggambarkan bahawa pemangkin mempunyai morfologi mikrozarah dengan ciri berliang. Bioarang terdop N yang disintesis pada 800 °C (N-800) menunjukkan prestasi terbaik dengan penyingkiran 98% AO7 dalam 30 min (pemalar kadar pseudo tertib pertama, $k_{app} = 0.211 \text{ min}^{-1}$). Didapati k_{app} meningkat dengan peningkatan dos PMS dan pemuatan N-800 manakala pH 7 merupakan pH terbaik bagi penyingkiran AO7. Kajian mengunakan perencat radikal natrium azida (NaN₃) menunjukkan bahawa oksigen singlet (1 O₂) adalah spesies oksigen reaktif (ROS) yang dominan dalam sistem tindak

Gasim et al.: PEROXYMONOSULFATE ACTIVATION USING NITROGEN-DOPED BIOCHAR FOR ACID ORANGE 7 REMOVAL IN WATER

balas ini. Prestasi pemangkin N-800 dalam penyingkiran AO7 telah berkurangan daripada 97 kepada 22% selepas empat kitaran berturut-turut disebabkan oleh penjerapan tidak berbalik dan pengoksidaan tapak aktif. Secara keseluruhan, N-800 dapat mengaktifkan PMS dengan berkesan dan menunjukkan potensi penyingkiran pewarna azo yang mampan. Dalam masa hadapan, pendopan bioarang terdop N terbitan plastik bersama heteroatom lain (seperti S, B) perlu disiasat untuk kesan sinergistik.

Kata kunci: proses pengoksidaan lanjutan, peroksimonosulfat, asid oren 7, nitrogen terdop, bioarang

Introduction

Industrialization and population development led to an increase in the usage of water and water pollution. This is predicated on the quality of the water deteriorating and the quantity of hydric resources decreasing, and the world is expected to experience a 40% water shortage by 2030 [1]. Synthetic dyes are widely employed in a variety of industries. Azo dyes are common dyes used in this dyeing industry. Due to the tremendous demand in diverse industries such as pulp and paper, textiles, pharmaceuticals and photo-electrochemical cells, huge amounts of azo dyes are produced globally (about 1 million tons per year) [2]. Acid orange 7 (AO7) is a commonly recognized azo dye since it is low in cost and can be applied rapidly in weakly acidic solutions. Exposure to AO7 has adverse health effects and its consumption is potentially lethal as it is carcinogenic and mutagenic [3]. There are several ways to eliminate AO7 from wastewater including adsorption, biodegradation, and advanced oxidation processes (AOPs). AOPs are chemical treatment procedures designed to remove organic and inorganic materials in wastewater.

Recently, persulfate-based advanced oxidation processes (PS-AOPs) emerged as a viable option for the decontamination of organics in water [1]. The activation of PS can yield strong oxidative species such as sulfate radical (SO₄-), hydroxyl radical (OH) and singlet oxygen (1O2) [4, 5]. These reactive species can be employed to decompose organic pollutants in wastewater. PS is commercially available peroxymonosulfate (PMS) and peroxydisulfate (PDS) depending on the number of SO₃ groups in its structure. Heterogenous catalytic activation of PS is highly preferred over other methods (e.g. heat activation, photoactivation) as no external energy sources are required, making heterogenous catalytic PS activation an economic choice [6]. Between PMS and PDS, the former is more easily activated due to it asymmetricity of structure [7]. Also, PMS is cheaper than PDS [8] making PMS a more advantageous choice of PS to be activated for organic pollutants degradation. Metalbased catalysts are effective in activating PMS, however, the inevitable leaching of metallic ions requiring the need for secondary treatment is a serious drawback [9]. Hence, carbon-based catalysts are emerging as sustainable alternatives. Carbon-based catalysts have preferable characteristics such as excellent specific surface area, microporosity, pore volume, chemical inertness, and stability. Examples of carbon-based catalysts are carbon nanotubes (CNTs), graphene, biochar and nanodiamonds. Among all, biochar is considered as the most economically viable option as it can be prepared directly from biomass waste. The catalytic activity of biochar can be increased by doping with a heteroatom such as nitrogen, sulfur and phosphorus [10]. N is the most compatible heteroatom dopant compared to others (e.g., B, S, P) due to its similar atom size with carbon, high electronegativity, and ability to provide effective active sites for PMS activation [10]. Moreover, the physiochemical properties of the biochar (i.e. thermal stability, functional groups) and the bonding configuration of the N-dopants are dependent on the synthesis temperature of the biochar [11]. These changes affect the overall catalytic performance of the N-doped biochar. Therefore, it is pivotal to study the effects of the synthesis temperature on the catalytic activity of Ndoped biochar for PMS activation.

In this study, we aim to prepare and investigate the characteristics of N-doped plastic-derived biochar at different pyrolysis temperatures (600, 700, and 800 °C). Thereafter, the catalytic performance of the as-prepared N-doped carbon-based catalysts was evaluated as PMS activator for AO7 degradation. The effects of different operational condition (i.e., PMS dosage, catalyst loading, pH) on AO7 removal via PMS activation were evaluated. Chemical scavenging study was employed to

investigate the mechanism of PMS activation by N-doped biochar. Lastly, the reusability of the catalyst was investigated.

Materials and Methods

Chemicals

The disposable vinyl gloves were purchased and used as the precursor in this study. The chemicals employed in this study were urea (QRëC), PMS (as Oxone®, 2KHSO₅·KHSO₄·K₂SO₄, Acros Organics), AO7 (Sigma-Aldrich), sodium hydroxide (NaOH, Fisher Chemical), ethanol (EtOH, 99.7%, QRëC), sodium perchlorate (NaClO₄, Sigma-Aldrich), tert-butyl alcohol (TBA, Supelco), and sodium azide (NaN₃, Merck). All experiments were carried out with deionized (DI) water.

Synthesis of N-doped biochar

In this study, the N-doped biochar was synthesized from disposable plastic gloves using a simple one-pot pyrolysis method. Firstly, the plastic gloves were cut into dimension of 1.4×1.4 cm, rinsed several times using DI water and dried in an oven at 60 °C. Then, the gloves and urea were mixed at a weight ratio of 1:2 (3g of gloves with 6g of urea), respectively, and the mixture was transferred into a crucible. The crucible was closed tightly and wrapped with aluminum foil to produce an oxygen limited atmosphere. Thereafter, the crucible was placed in the furnace (Carbolite Gero Ltd.) and heated to a selected temperature with a heating rate of 10 °C min⁻¹ for 2 h. The calcination temperature was varied from 600, 700 to 800 °C. Thereafter, the resultant Ndoped biochar was allowed to cool under room temperature, washed several times with DI water and dried in an oven at 60 °C. The resultant N-doped biochar was labelled as N-600, N-700, and N-800 according to the calcination temperature.

Characterization

The attenuated total reflectance-Fourier transform infrared (ATR-FTIR) spectroscopy (Frontier, Perkin Elmer) was used for the determination of the functional groups of N-doped biochar. The crystal structure/s of the as-prepared N-doped biochar samples were analyzed using the powder X-ray diffraction (XRD) patterns (Bruker D8 Advance diffractometer). Field Emission Scanning Electron Microscope (FESEM, Quanta

FEG650, FEI) equipped with energy dispersive X-ray spectroscopy (EDX) were used to analyze the samples' surface morphologies and elemental composition. Thermogravimetric analysis (TGA) was conducted using PerkinElmer thermal analyzer in nitrogen atmosphere (ramping rate = 10 °C min⁻¹) to analyze the thermal properties of the as-prepared N-doped biochar samples.

Catalytic performance evaluation

Briefly, a solution containing PMS (0.2 g L⁻¹) and AO7 (10 mg L⁻¹) was prepared in a 250 mL reaction vessel (mole ratio of PMS:AO7 of 1:23). To initiate the catalytic degradation, 0.025 g L⁻¹ of the N-doped biochar catalyst was added into the solution mixture mentioned above. At 5 min intervals, 3 mL aliquots of the solution were drawn from the solution and filtered using $0.45 \mu m$ cellulose acetate filter to remove the catalyst particles and avoid misleading results. The concentration of AO7 was determined by a calibration curve using a UV-Vis spectrophotometer (Shimadzu 2600 UV–Vis) at $\lambda = 485$ nm. The effects of various operating parameters including initial pH (3-9), catalyst loading (0.01-0.1 g L⁻ 1) and PMS dosage (0.1-0.25 g L⁻¹) for AO7 degradation were also studied. To identify the dominant ROS, chemical scavengers were used. TBA (30 mM), NaN₃ (3 mM), NaClO₄ (485 mM) and EtOH (2 M), were used as scavengers for 'OH, 1O2, nonradical electron-transfer, and both SO₄ and OH, respectively. The degradation tests were performed in duplicates to ensure reproducible results. The reusability of N-800 was studied by conducting four consecutive catalytic cycles in which the N-doped biochar catalyst was recovered using gravitational method, dried and scaled out after each cycle and reused. The total organic carbon (TOC) removal of AO7 by N-800 was measured by using a TOC analyzer (Shimadzu TOC-VCPH).

Results and Discussion

Characterization of biochar catalyst

The crystal structure of the as-synthesized N-800 was investigated using XRD and the results are presented in Figure 1a. In general, the presence of short-range order in the carbon structure is characterized by diffuse and broad bands in XRD patterns, whereas highly crystalline phases with a high degree of long-range order are

Gasim et al.: PEROXYMONOSULFATE ACTIVATION USING NITROGEN-DOPED BIOCHAR FOR ACID ORANGE 7 REMOVAL IN WATER

confirmed by sharp and distinct peaks. Notably, several diffraction peaks typical of amorphous carbon can be observed at $2\theta = 26.2^{\circ}$ and 43.9° , representing the (002) and (101) planes, respectively, for N-800. These two planes show the presence of amorphous carbon after the pyrolysis suggesting that the plastic residue has been successfully carbonized into biochar [9]. Apparently, the diffraction peak at $2\theta = 26^{\circ}$ shows the presence of a crystalline phase with a well-ordered structure produced

through calcination and N-doping [12,13]. A sharp peak at $2\theta = 29^{\circ}$ indicating the existence of crystalline inorganic elements which can be identified as calcium (CaCO₃) in plastic residue [14]. The presence of Ca was minimally present in EDX mapping. Other researchers that studied the pyrolysis of other wastes also noted the existence of inorganic elements [15]. Overall, the result showed that the biochar was successfully synthesized.

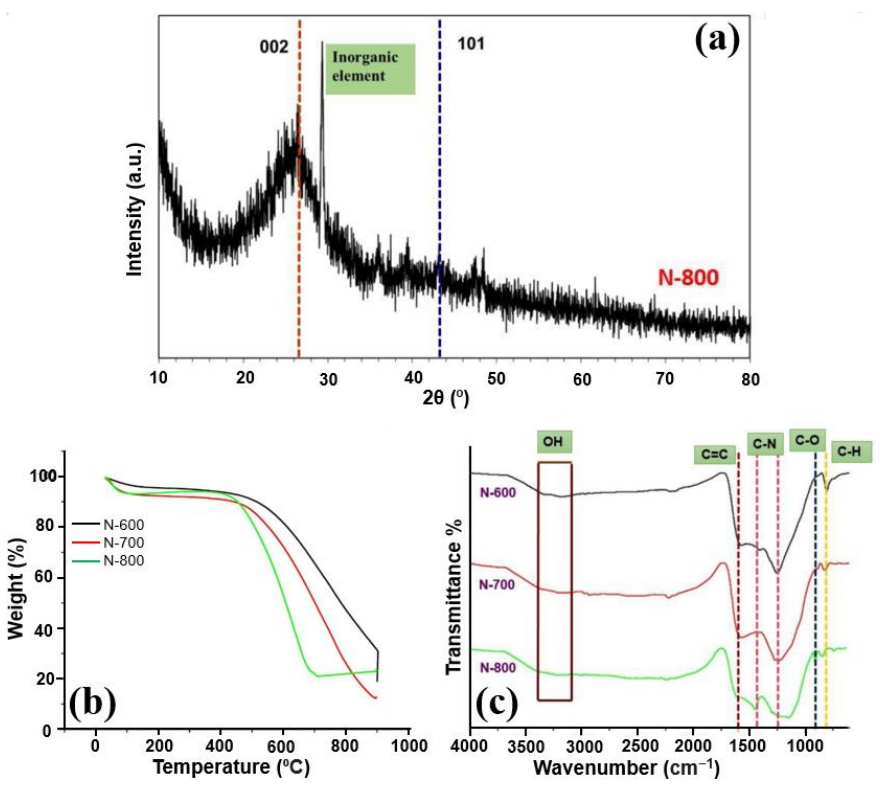


Figure 1. (a) XRD diffractogram, (b) TGA patterns, and (c) FTIR spectra of the as-prepared catalysts

The TGA analysis was carried out to evaluate the thermal stability of N-600, N-700, and N-800 by observing the weight change of the samples with respect to increasing temperature (Figure 1b). All the TGA curves displayed an initial weight loss between 10-30% corresponding to the evaporation of the adsorbed H₂O molecules. There is a continuous drop in weight over a wide temperature range between 500 to 900 °C. Generally, N doping may improve heat tolerance in contrast to normal carbon biochar since N doping induced greater thermodynamic stability of the catalyst against combustion reaction [12]. Furthermore, a larger

percent weight/weight inorganic content, which primarily consists of Ca, could increase the proportion of inert components in the carbocatalyst, reducing overall catalytic activity.

The functional groups in the N-doped biochar were analyzed using FTIR and the results are illustrated in Figure 1c. The presence of an absorbance peak at 3250 cm⁻¹ is observed signifying -OH bond from hydroxyl and carboxylic groups, and adsorbed water [16]. The broad peaks at the range of 950-1100 cm⁻¹ show C-O bond of hydroxyl and alkoxy groups [17]. Several peaks

have appeared at the range of 740-825 cm⁻¹ after the thermal treatment indicating the presence of C-H bending vibration (aromatic) while the peak at 1500 cm⁻¹ shows that C=C bonding is present. This bonding denotes a higher degree of graphitization [18,19]. Two broad peaks form at 1185 cm⁻¹ and 1381 cm⁻¹ which shows C-N bond due to the doping of N on the catalyst [20].

The structure and elemental mapping of the synthesized N-800 were characterized using FESEM-EDX (Figure 2). It was observed that N-800 has a morphology consisting of microparticles with porous features. The N-800 displayed a dispersive pore structure making it an effective platform for adsorption and catalysis [10]. The

exterior surface of N-800 illustrated roughness with wrinkles and folds suggesting that N doping procedure caused the creation of defective sites. Other than that, N-800 has smooth interior surface indicating that N-doping is limited to the external surface. A possible reason might be the N-doping method where the urea acting as nitrogen precursor will be unable to diffuse into the interior pores implying that adjusting particle size could improve the surface coverage of N species [12]. Besides that, the elemental mapping shows that the N and O atoms are uniformly distributed on N-800. The presence of Ca was also detected in EDX analysis albeit at lower concentration.

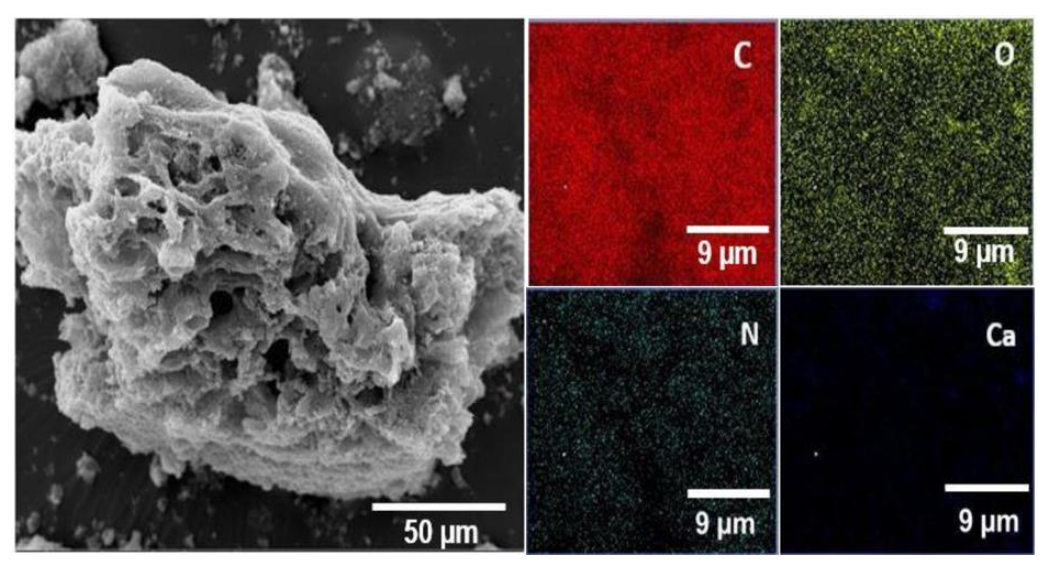


Figure 2. SEM image and elemental mapping of N-800.

Catalytic performance of different catalysts

Figure 3a shows the effect of synthesis temperature of N-doped biochar on the performance of AO7 removal by PMS activation. The control study shows that the AO7 adsorption at 30 min was ~32%. Notably, almost no AO7 degradation was observed in the presence of PMS alone indicating that AO7 is stable to direct PMS oxidation. However, when PMS was activated in presence of N-600, N-700, and N-800, rapid AO7 degradation can be observed. The AO7 degradation by N-doped biochar was evaluated using the pseudo first order kinetics as follows:

$$[AO7]_t = [AO7]_0 e^{-kapp t}$$
 (1)

where [AO7]_t, [AO7]₀, and k_{app} are the AO7 concentration at selected time interval, initial AO7 concentration, and pseudo-first order rate constant (min
1), respectively. Apparently, N-800 displays the best catalytic performance where degradation efficiency of AO7 reached 98% in 30 min while N-600 shows the slowest AO7 removal with only 75% of AO7 removed in 30 min. The obtained k_{app} was in order: N-600 ($k_{app} = 0.044 \, \text{min}^{-1}$) < N-700 ($k_{app} = 0.083 \, \text{min}^{-1}$) < N-800 ($k_{app} = 0.211 \, \text{min}^{-1}$). While higher calcination temperature will cause the C-N bond to break resulting in the loss of nitrogen, it promotes incorporation of N atoms into the graphitic carbon network as graphitic N [21]. The

graphitic N has been previously identified as the main active site for PMS activation. Hence, N-800 was used in additional degradation studies since it demonstrated

the greatest catalytic performance to activate PMS for AO7 degradation.

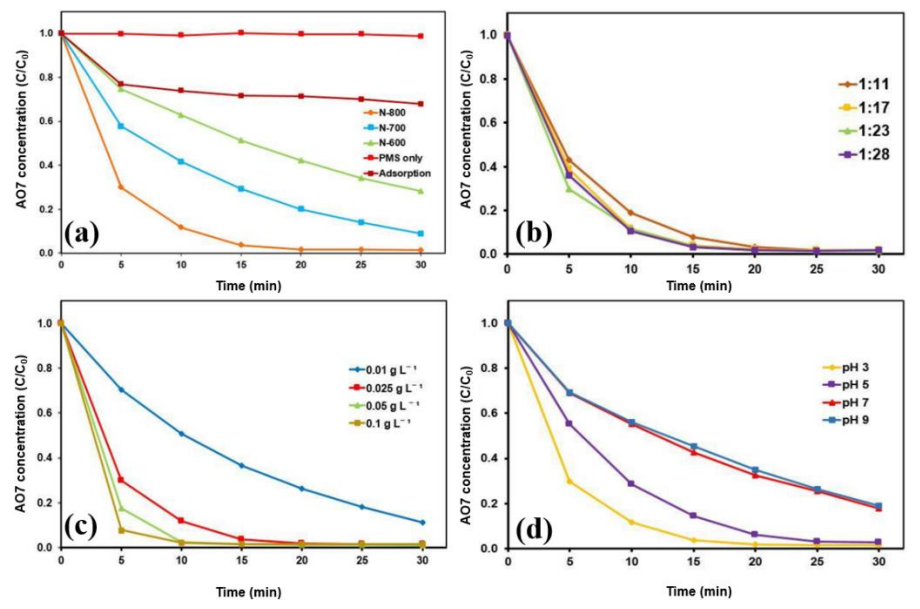


Figure 3. (a) Catalytic degradation of AO7 by different catalysts. Effects of (b) AO7:PMS ratio, (c) catalyst loading, and (d) initial pH

Effect of reaction parameters

Figure 3b shows the effect of PMS dosage on AO7 removal. The k_{app} increased when the ratio of AO7:PMS was decreased in following order: [0.1 g L⁻¹ of PMS] 1:11 $(k_{app} = 0.155 \text{ min}^{-1}) < [0.15 \text{ g L}^{-1} \text{ of PMS}] 1:17 (k_{app})$ = 0.161 min⁻¹) < [0.20 g L⁻¹ of PMS] 1:23 (k_{app} = 0.170 min-1). However, when the ratio of AO7:PMS was decreased from 1:23 to 1:28 [0.25 g L⁻¹ of PMS], the k_{app} decreased to 0.168 min⁻¹. From these results, it can be observed that 1:23 of AO7: PMS shows the highest AO7 degradation rate and optimum rate for AO7 removal. Usually, higher PMS dosage can promote greater interaction between catalyst and PMS for effective AO7 degradation. However, the rate decreased slightly when AO7: PMS was decreased to 1:28 due to the SO4*consumption by excessive PMS leading to unproductive SO4 use. Excessive PMS could scavenge SO4 and produce less reactive SO₅*- (Eq. (2)) [22].

$$HSO_5^- + SO_4^{\bullet-} \rightarrow SO_5^{\bullet-} + SO_4^{2-} + H^+$$
 (2)

Figure 3c shows the effect of catalyst loading on the AO7 removal. The degradation efficiency and rate increased linearly with increasing catalyst loading in the following order: 0.01 g L⁻¹ ($k_{app} = 0.067 \text{ min}^{-1}$) < 0.025 g L⁻¹ $(k_{app} = 0.211 \text{ min}^{-1}) < 0.05 \text{ g L}^{-1} (k_{app} = 0.260 \text{ min}^{-1})$ ¹) < 0.1 g L⁻¹ ($k_{app} = 0.264 \text{ min}^{-1}$). Increasing the catalyst loading increases the concentration of active sites available for PMS activation to produce ROS for AO7 degradation [12,23]. As the catalyst can be reused, modifying the catalyst loading is a more effective strategy to manage the reaction than adjusting PMS dosage. The effect of pH on the degradation of AO7 is presented in Figure 3d. From the figure, the catalytic activity of N-800 is much better achieved under acidic conditions compared with neutral and alkaline conditions. The k_{app} for AO7 removal increased in the following order: pH 3 ($k_{app} = 0.170 \text{ min}^{-1}$) > pH 5 ($k_{app} =$ 0.130 min^{-1}) > pH 7 ($k_{app} = 0.057 \text{ min}^{-1}$) > pH 9 (k_{app} =0.054 min⁻¹). This observation might be due to the repulsion effect between the surface of the catalyst $(pH_{pzc} = 7.4)$, AO7 (pKa = 10.7) and PMS $(pKa_2 = 9.4)$ [12,23]. Both radical and nonradical routes require PMS

to be in contact with the surface of the catalyst to facilitate the direct electron transfer process. Therefore, this surface repulsion will be detrimental to the reaction, decreasing the overall rate of degradation of AO7 [24,25]. Moreover, the initial pH may have an impact on how much AO7 is adsorbed by the catalyst, causing it to adsorb more AO7 in moderately acidic conditions and increasing the AO7 degradation rate [26].

Identification reactive species and possible catalytic mechanism

For PMS activation using carbocatalysts, there are two activation pathways that have been reported which are the radical and nonradical pathways. These pathways have an impact on the system's performance. Chemical scavengers such as EtOH, TBA, NaN₃ and NaClO₄ were used to identify the dominant ROS. EtOH was used to selectively scavenge 'OH and SO₄'- ($k_{\text{SO4-+EtOH}} = 1.6 \times 10^7 \,\text{M}^{-1} \,\text{s}^{-1}$; $k_{\text{+OH+EtOH}} = 1.9 \times 10^9 \,\text{M}^{-1} \,\text{s}^{-1}$) [12]. As shown in Figure 4, the addition of EtOH into the reaction system shows 48% inhibition and reduced the k_{app} from 0.170 min⁻¹ to 0.088 min⁻¹. This suggests that SO₄'- and

'OH might be involved in degradation of AO7. To determine the dominant radical, TBA was used to quench 'OH because TBA has larger value of reaction rate constant with 'OH compared to SO_4 ' ($k_{SO4-+TBA}$ = $4-9.1 \times 10^5 \,\mathrm{M}^{-1} \,\mathrm{s}^{-1}$, $k_{\bullet \mathrm{OH}+\mathrm{TBA}} = 3.8-7.6 \times 10^8 \,\mathrm{M}^{-1} \,\mathrm{s}^{-1}$) [12]. TBA shows a minor inhibitory effect in this reaction system. This suggests that the involvement of 'OH was limited in degradation of AO7. Next, NaClO4 was employed to reduce the interaction between the catalyst and PMS which decreases the formation of surface complexes for the nonradical pathway. NaClO₄ addition into the reaction system shows a 30% inhibition and reduced the k_{app} from 0.170 min⁻¹ to 0.119 min⁻¹. NaClO₄ can reduce the amount of the nonradical pathway without significantly influencing the radical pathway because it can hinder the surface contact between PMS and the catalyst [27]. Finally, NaN3 is used to scavenge ¹O₂. When NaN₃ was employed, the percentage of inhibition was 80% and k_{app} was reduced from 0.170 min⁻¹ to 0.034 min⁻¹. The highest inhibitory effect shown by the NaN₃ signifies that ¹O₂ was dominant in the system.

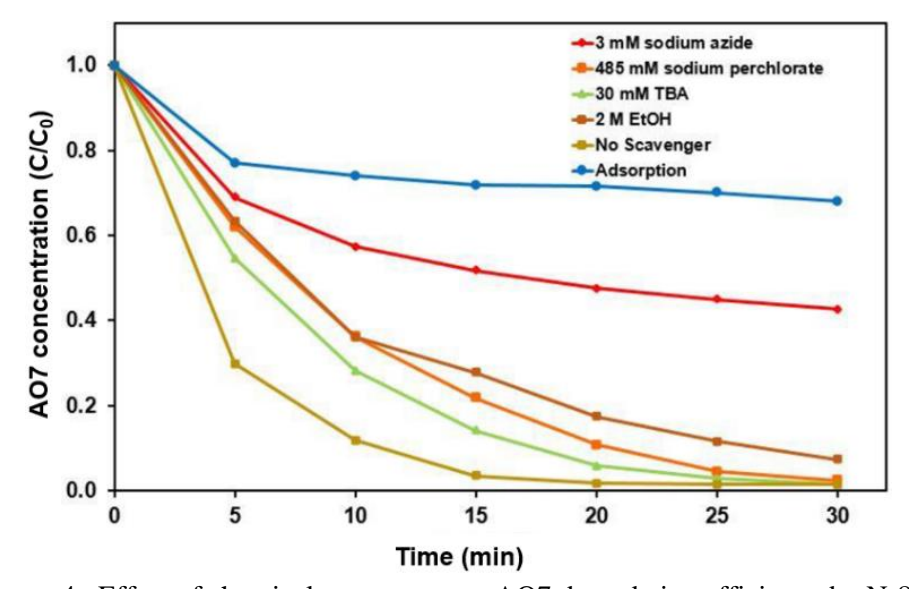


Figure 4. Effect of chemical scavengers on AO7 degradation efficiency by N-800

The results show that there was coexistence between radical and nonradical pathway in this system. Sun et al. proposed that the radical route occurs when the abundant free-flowing electrons from sp^2 carbons conjugate with the lone-pair electrons of N dopants

found at Lewis basic sites containing lone-pair electrons such as pyridinic N, pyrrolic N, and ketonic groups. These functional groups can operate as electron donors, transferring electrons to activate PMS by cleaving the O-O bond resulting in production of SO₄*- and 'OH

Gasim et al.: PEROXYMONOSULFATE ACTIVATION USING NITROGEN-DOPED BIOCHAR FOR ACID ORANGE 7 REMOVAL IN WATER

[28,29]. Oh et al. proposed that N-doped biochar from biomass waste can be considered as an optimal surface for electron transfer reactions to take place since it has a high concentration of graphitic N and sp^2 hybridized carbon. An electron-deficient environment for the carbon atom is produced when the highly electronegative N atom in the graphitic plane attracts an electron from the less electronegative carbon next to it. Through an electron abstraction process, the electron-deficient carbon may interact strongly with PMS,

resulting in the production of 1O_2 [30]. The overall results are in consistent with this observation. Hence, it can be speculated that Lewis base group like pyridinic N, pyrrolic N and ketonic groups involved in free radical pathway, while 1O_2 formation involves in PMS activation by electron deficient carbon induced by the graphitic N (dominant). The mechanism of PMS activation by N-doped plastic-derived biochar for AO7 degradation is illustrated in Figure 5.

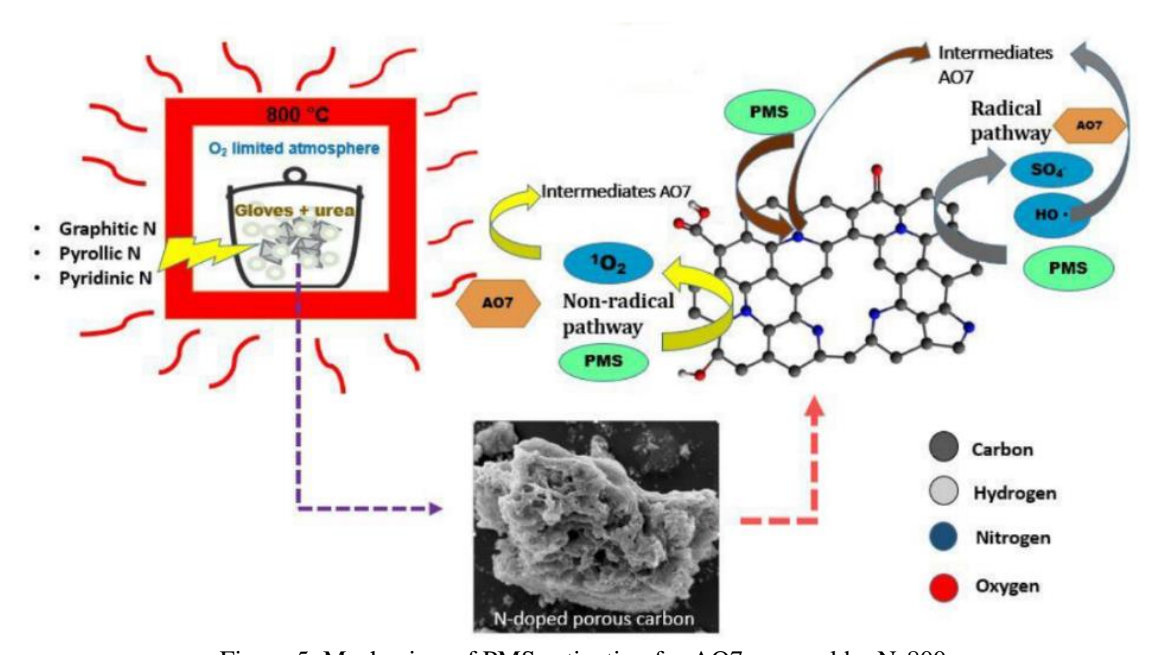


Figure 5. Mechanism of PMS activation for AO7 removal by N-800

Reusability of N-800

In practical applications, stability of N-800 in the PMS system for degradation of pollutant is important. The degradation of AO7 was carried out 4 times using recycled N-800 biochar and the results are presented in Figure 6. In the first cycle, the degradation rate was 97% in 30 min. The removal efficiency was reduced to 89%, 56%, 22% within 30 min in the second, third and fourth cycles, respectively. The N-800 deactivation could be ascribed to the change of configuration of nitrogen bonding and intermediates coverage of catalyst which

blocked the PMS interaction with active sites and minimized production of ROS [21]. In short, the N-800 can still efficiently remove AO7 after being used repeatedly. TOC removal of ~5% was achieved in the first 60 min of the oxidation reaction. After 3h, TOC removal reached a 10% suggesting that AO7 can be mineralized by the oxidation processes (Eq. (3)) provided that prolong treatment time was employed.

$$AO7 + ROS \rightarrow CO_2 + H_2O + inorganic ions$$
 (3)

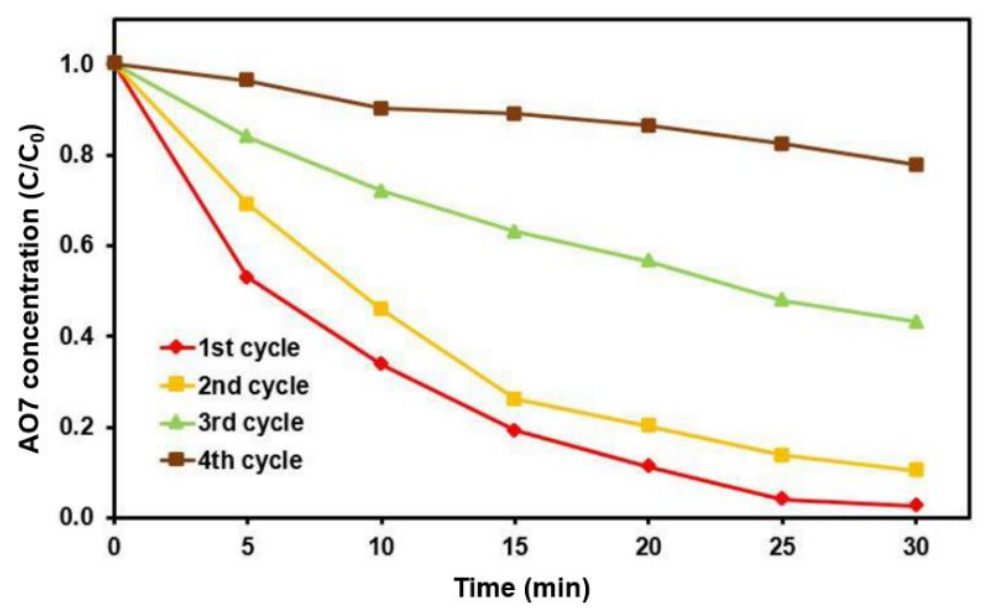


Figure 6. Reusability of N-800 in AO7 removal

Conclusion

In conclusion, N-doped biochar was successfully synthesized by utilizing a thermal calcination approach in an oxygen-limited environment for AO7 degradation by PMS activation. The obtained FTIR spectra of all Ndoped biochar and XRD patterns of N-800 proved that the catalysts were successfully synthesized in this study. Through FESEM-EDX, it can be confirmed that N-800 consisted of microparticles with a porous feature with uniform distribution of the N atoms. From effect of synthesis temperature on the performance of AO7 removal by PMS activation, N-800 exhibited the highest efficiency in degrading AO7 and was used for further degradation experiments. About 98% of AO7 was successfully eliminated within 30 min employing N-800/PMS. The catalytic activity of N-800 in terms of PMS activation for AO7 removal with various operating variables (i.e. initial pH, catalyst loading, and PMS dosage) were investigated. The k_{app} values were found to be increasing with the increasing catalyst loading. An AO7: PMS ratio of 1:23 was found to be the optimum ratio for the degradation of AO7. The lower dosage of PMS lowered the k_{app} due to the limited PMS molecules available for activation and ROS formation. Excessively higher dosage of PMS also lowered the k_{app} because it could scavenge SO₄. and produce less reactive SO₅. On the other hand, the study on initial pH indicated that the ideal operating pH is found in acidic conditions. This can be explained by the surface repulsion between catalyst, PMS and AO7 at alkaline pH. The TOC removal efficiency by using N-800 was 10% indicating that mineralization of AO7 was achieved. Moreover, the catalyst was able to be reused for four consecutive cycles. Scavenger studies showed that the ¹O₂ pathway was the prevailing pathway in the degradation of AO7. Overall, it can be inferred that SR-AOPs is a promising technology which can be used effectively to treat organic contaminants in the wastewater.

Acknowledgement

The authors would like to acknowledge the financial support provided by the Ministry of Higher Education Malaysia for Fundamental Research Grant Scheme (FRGS) with project code: FRGS/1/2020/STG04/USM/02/2.

References

- Guerra-Rodríguez, S., Rodríguez, E., Singh, D. N. and Rodríguez-Chueca, J. (2018). Assessment of sulfate radical-based advanced oxidation processes for water and wastewater treatment: a review. *Water (Switzerland)*, 10(12): 1828.
- 2. Swain, G., Singh, S., Sonwani, R. K., Singh, R. S., Jaiswal, R. P. and Rai, B.N. (2021). Removal of

- acid orange 7 dye in a packed bed bioreactor: process optimization using response surface methodology and kinetic study. *Bioresource Technology Reports*, 13: 100620.
- 3. Perera, H. J. (2020). Removal of acid orange 7 dye from wastewater: review. *Advances in Science and Engineering Technology International Conferences*, pp. 1-6.
- 4. Oh, W. Da, Dong, Z. and Lim, T. T. (2016). Generation of sulfate radical through heterogeneous catalysis for organic contaminants removal: current development, challenges and prospects. *Applied Catalysis B: Environmental* 194: 169-201.
- Xia, X., Zhu, F., Li, J., Yang, H., Wei, L., Li, Q., Jiang, J., Zhang, G. and Zhao, Q. (2020). A Review study on sulfate-radical-based advanced oxidation processes for domestic/industrial wastewater treatment: degradation, efficiency, and mechanism. Frontiers in Chemistry 8: 1092.
- Gasim, M. F., Veksha, A., Lisak, G., Low, S.C., Hamidon, T.S., Hussin, M.H. and Oh, W. Da (2023). Importance of carbon structure for nitrogen and sulfur co-doping to promote superior ciprofloxacin removal via peroxymonosulfate activation. *Journal of Colloid and Interface Science*, 634: 586-600.
- Song, H., Yan, L., Wang, Y., Jiang, J., Ma, J., Li, C., Wang, G., Gu, J. and Liu, P. (2020). Electrochemically activated PMS and PDS: Radical oxidation versus nonradical oxidation. *Chemical Engineering Journal*, 391: 123560.
- 8. Gasim, M. F., Choong, Z. Y., Koo, P. L., Low, S. C., Abdurahman, M. H., Ho, Y. C., Mohamad, M., Suryawan, I. W. K., Lim, J. W. and Oh, W. Da (2022). Application of biochar as functional material for remediation of organic pollutants in water: an overview. *Catalysts*, 12(2): 210.
- Wang, J., Cai, J., Wang, S., Zhou, X., Ding, X., Ali, J., Zheng, L., Wang, S., Yang, L., Xi, S. et al. (2022). Biochar-based activation of peroxide: multivariate-controlled performance, modulatory surface reactive sites and tunable oxidative species. *Chemical Engineering Journal*, 428: 131233.
- 10. Han, R., Fang, Y., Sun, P., Xie, K., Zhai, Z., Liu, H. and Liu, H. (2021). N-doped biochar as a new metal-free activator of peroxymonosulfate for

- singlet oxygen-dominated catalytic degradation of acid orange 7. *Nanomaterials*, 11(9): 2288.
- 11. Gasim, M. F., Lim, J.-W., Low, S.-C., Lin, K.-Y.A. and Oh, W.-D. (2022). Can biochar and hydrochar be used as sustainable catalyst for persulfate activation? *Chemosphere*, 287: 132458.
- Oh, W. Da, Veksha, A., Chen, X., Adnan, R., Lim, J. W., Leong, K. H. and Lim, T.T. (2019). Catalytically active nitrogen-doped porous carbon derived from biowastes for organics removal via peroxymonosulfate activation. *Chemical Engineering Journal*, 374: 947-957.
- Ungár, T., Gubicza, J., Ribárik, G., Pantea, C. and Zerda, T. W. (2002). Microstructure of carbon blacks determined by X-ray diffraction profile analysis. *Carbon*, 40(6): 929-937.
- Ng, W.-Y., Choong, Z.-Y., Gasim, M. F., Khoerunnisa, F., Lin, K.-Y.A. and Oh, W.-D. (2002). Insights into the performance and kinetics of face mask-derived nitrogen-doped porous carbon as peroxymonosulfate activator for gatifloxacin removal. *Journal of Water Process Engineering*, 50: 103239.
- 15. Lawrinenko, M. and Laird, D. A. (2015). Anion exchange capacity of biochar. *Green Chemistry*, 17(9): 4628-4636.
- Guo, D., Xin, R., Wang, Y., Jiang, W., Gao, Q., Hu, G. and Fan, M. (2019). N-doped carbons with hierarchically micro- and mesoporous structure derived from sawdust for high performance supercapacitors. *Microporous and Mesoporous Materials*, 279: 323-333.
- 17. Dey, R. S., Hajra, S., Sahu, R. K., Raj, C. R. and Panigrahi, M. K. (2012). A rapid room temperature chemical route for the synthesis of graphene: metalmediated reduction of graphene oxide. *Chemical Communications*, 48(12): 1787-1789.
- 18. Liu, N., Zhang, Y., Xu, C., Liu, P., Lv, J., Liu, Y.Y. and Wang, Q. (2020). Removal mechanisms of aqueous Cr(VI) using apple wood biochar: a spectroscopic study. *Journal of Hazardous Materials*, 384: 121371.
- 19. Yu, J., Tang, L., Pang, Y., Zeng, G., Wang, J., Deng, Y., Liu, Y., Feng, H., Chen, S. and Ren, X. (2019). Magnetic nitrogen-doped sludge-derived biochar catalysts for persulfate activation: Internal

- electron transfer mechanism. *Chemical Engineering Journal*, 364: 146-159.
- Maiyalagan, T. and Viswanathan, B. (2005).
 Template synthesis and characterization of well-aligned nitrogen containing carbon nanotubes.
 Materials Chemistry and Physics, 93(2-3): 291-295.
- 21. Xu, L., Wu, C., Liu, P., Bai, X., Du, X., Jin, P., Yang, L., Jin, X., Shi, X. and Wang, Y. (2020) Peroxymonosulfate activation by nitrogen-doped biochar from sawdust for the efficient degradation of organic pollutants. *Chemical Engineering Journal*, 387: 124065.
- Fan, Y., Zhou, Z., Feng, Y., Zhou, Y., Wen, L. and Shih, K. (2020). Degradation mechanisms of ofloxacin and cefazolin using peroxymonosulfate activated by reduced graphene oxide-CoFe₂O₄ composites. *Chemical Engineering Journal*, 383: 123056.
- Li, Z., Sun, Y., Yang, Y., Han, Y., Wang, T., Chen, J. and Tsang, D.C.W. (2020). Biochar-supported nanoscale zero-valent iron as an efficient catalyst for organic degradation in groundwater. *Journal of Hazardous Materials*, 383: 121240.
- 24. Zhang, T., Zhu, H. and Croué, J. P. (2013). Production of sulfate radical from peroxymonosulfate induced by a magnetically separable CuFe₂O₄ spinel in water: Efficiency, stability, and mechanism. *Environmental Science and Technology*, 47(6): 2784-2791.
- 25. Pérez-Urquiza, M. and Beltrán, J. L. (2001). Determination of the dissociation constants of sulfonated azo dyes by capillary zone electrophoresis and spectrophotometry methods. *Journal of Chromatography A* 917(1–2): 331-336.

- Khan, R., Habib, M., Gondal, M. A., Guan, K., Zhou, P., Zhang, J. and Zhu, L. (2020). Catalytic degradation of acid orange 7 in water by persulfate activated with CuFe₂O₄@RSDBC. *Materials Research Express*, 7(1): 016529.
- 27. Zaeni, J. R. J., Lim, J. W., Wang, Z., Ding, D., Chua, Y. S., Ng, S. L. and Oh, W. Da (2020). *In situ* nitrogen functionalization of biochar via one-pot synthesis for catalytic peroxymonosulfate activation: characteristics and performance studies. *Separation and Purification Technology*, 241: 116702.
- 28. Sun, P., Liu, H., Feng, M., Guo, L., Zhai, Z., Fang, Y., Zhang, X. and Sharma, V. K. (2019). Nitrogensulfur co-doped industrial graphene as an efficient peroxymonosulfate activator: singlet oxygendominated catalytic degradation of organic contaminants. *Applied Catalysis B: Environmental*, 251: 335-345.
- Sun, H., Peng, X., Zhang, S., Liu, S., Xiong, Y., Tian, S. and Fang, J. (2017). Activation of peroxymonosulfate by nitrogen-functionalized sludge carbon for efficient degradation of organic pollutants in water. *Bioresource Technology*, 241: 244-251.
- 30. Chen, X., Oh, W. Da, Hu, Z. T., Sun, Y. M., Webster, R. D., Li, S. Z. and Lim, T. T. (2018). Enhancing sulfacetamide degradation by peroxymonosulfate activation with n-doped graphene produced through delicately-controlled nitrogen functionalization via tweaking thermal annealing processes. *Applied Catalysis B: Environmental*, 225: 243-257.